STATIC AND ON-LINE EARTHQUAKE RESPONSE TESTS ON 3 STORY FRAME OF A LOW-YIELD-RATIO STEEL

(I) (II)
Koichi Takanashi, Ling-hua Meng,
Boris Simeonov (III)

INTRODUCTION

Structural materials, preferable for earthquake resistant structures are expected to show deformation capacity as well as high strength. Recently steel makers began to produce rather ideal steels by modern steel-making technology, where neatly controlled rolling process are conducted. This paper describes pilot tests which were carried out aiming at proof of applicability of such a new steel to building structures. There were two types of tests conducted ; static tests and earthquake response tests by the on-line test control technique. At first the static tests on 3 story moment resistant frames are described. The strength and the deformation capacity under static and monotonically increasing loads are discussed referring to test results. Then, earthquake response behavior of identically designed frames in the elastic and plastic range obtained by the on-line tests are presented.

TEST STRUCTURES

Steel material Properties of steel materials, called tentatively here as New HT60 1), used in the tests were examined by coupon tests, and summarized in Table 1. A typical stress vs. strain diagram by the coupon tests are shown in Fig. 1. It is noticeable that rather steeper slope at the initiation of strain-hardening exists after shorter plastic plateau compared as stress-strain diagrams of ordinary mild steels. The yield ratio YR, namely δ_y / δ_u, are less than 80%. It is considered desirable at this moment.

Test frames A test frame is composed by a set of combination of member sections denoted as H6, H8 and H12. Section properties of the members are summarized in Table 2. The numerals after H mean the width to thickness ratios of the outstanding flange. These ratios guarantee formation of plastic hinges before onset of local buckling.

By help of preliminary plastic analyses of model frames under horizontal loads at floor levels, which linearly increase upward, four types of test frames were designed :

(I) Professor, Institute of Industrial Science, University of Tokyo, TOKYO,JAPAN

(II) Graduate student, University of Tokyo, TOKYO, JAPAN

(III) Professor, University "Kiril and Metodiji", SKOPJE, YUGOSLAVIA

WBSC-W-1 Weak beam, strong column type frame with weak panel at beam-to-column connection

WBSC-S-1 Weak beam, strong column type frame with strong panel

SBWC-W-1 Strong beam, weak column type frame with weak panel

SBWC-S-1 Strong beam, weak column type frame with strong panel

The elevations of test frames are presented in Fig. 2.

The plastic analyses by the simple plastic hinge method gave us story shears at the 1st to 3rd floors, Q_1 , Q_2 and Q_3 , at the instance of collapse for each frames. The values are summarized in Table 3. The associated collapse modes are shown in Fig. 3. In the analyses, the yield moment of the connection panels M_S were evaluated by $M_S = A_p t_p \tau_y$, where A_p is aspect area, t_p panel thickness and τ_y yield shear stress.

Test setup The loading system and the data acquisition system is schematically presented in Fig. 4. In the static tests, only the 3rd actuator was controlled by the stroke control signal from the computer, and the 1st and the 2nd actuators were so controlled by the load control signal according to prescribed parameters η_1 and η_2 that were fixed throughout a test. Loads were measured by load cells attached at the top of the actuators and horizontal displacements were measured by the displacement meters. All data were recorded into a data recorder, among which the loads and the horizontal displacements were input to the computer for determining control signals. In the on-line earthquake response tests, the load control system was a little modified as shown in Fig. 5. There, all actuators were controlled by the stroke signals, which were determined by the earthquake response displacements computed in the computer at each time step. The test procedure of the on-line earthquake response tests has been explained elsewhere 2).

STATIC TESTS

Story shear Q vs. story displacement δ diagrams in Fig. 6 were converted from load and displacement measurement data. In the figure, the calculated values by the limit analysis are shown as short lines. Loads were applied until the maximum load was attained except in the test of WBSC-W-1, where the loading was stopped because of the stroke limitation of an actuator. Thus, the maximum load of WBSC-W-1 is presumed by exterpolation. In order to examine the distribution of plastic deformation, the absorbed strain energy defined as $\int Q \, d\delta$ in each story was calculated from the test results. The total amounts of absorbed energy and the percentage of the shared energy by each story are summarized in Table 4. Bending moment vs. axial force interactions at the column bases are shown in Fig. 7.

Major findings in the static tests are as follows :
1) Stable load vs. displacement curves are obtained till the maximum loads.
2) Local buckling was observed, but it did not cause the loss of strength, because of strain-hardening.

3) The strength observed at the tests is much higher than the calculated strength which is calculated by the simple plastic analysis for perfectly plastic materials.
4) New approach must be developed to predict the strength in stead of the simple plastic analysis in the case that steel materials show rather strong strain-hardening.
5) The design concept of weak beam-strong column type frame is effective in distributing the strain energy absorption to prevent the concentration of structural damage.
6) Plastic hinges conformed at connection panels work effectively for the above mentioned purpose.

ON-LINE EARTHQUAKE RESPONSE TESTS

Frames identically designed as the frames in the static tests were then tested by the on-line test control method. As already presented elsewhere, 2) this method gives us earthquake response behavior without using shaking tables.

Ground acceleration In the test the ground acceleration wave form recorded in 1940 El Centro Earthquake (NS component) was used as the input acceleration. But the duration time is limited to 15 sec and the peak acceleration values are so adjusted to be related to the strength found in the static tests. The peak value A_{max} is determined by Eq. (1).

$$A_{max} = \alpha A_y \qquad (1)$$

where A_y = Q_u /(3M)
Q_u = Static strength
M = Mass at each floor
α = 1.2

The parameter α is fixed as 1.2 through all tests.

Dynamic parameters The period and the mass distribution can be given arbitrarily so as to make up a desirable frame model for response tests. In tests, the 1st natural period T_1 is fixed as T_1 = 0.80 sec. Accordingly, the value of mass, assumed same at all floor levels, was determined from the fixed period and the frame stiffness evaluated by preliminary static tests prior to the on-line response tests. The viscous damping factors, which are needed for integrating the equation of motion in the computer, are 0.02 as h_1 for the 1st mode vibration and $h_s = (\omega_s / \omega_1) h_1$ (s = 2,3). The time step in the numerical integration was 0.01 sec. All dynamic properties used in the tests are summarized in table 5.

Test results The on-line earthquake response tests were conducted on test frames WBSC-W-2, WBSC-S-2 and SBWC-W-2. The dimensions of these frames are same as those of the frames of identical codes in the static tests. Distribution of inertial forces induced at the mass positions during vibration are very important in order to replace it by the static load distribution in actual design procedures. Trajectories of the inertial forces at the 1st, 2nd and 3rd floors, F_1, F_2 and F_3, respectively, are shown in Fig. 8. Solid lines in the figures show the ratios between the loads applied at the floor levels in the static tests. Dashed lines show the ratios between the

floor levels in the static tests. Dashed lines show the ratios between the inertial forces induced during the 1st mode vibration. The story shear Q vs. the story displacement δ relationship observed in the tests are shown in Fig. 9, even though only the relations at the most damaged story in each test are selected. Time histories of response displacements at the top of each frame are shown in Fig. 10.

Major findings are as follows :

1) The trajectories of the inertial forces are crowded along the line representing the ratio between the inertial forces during the 1st mode vibration. It suggests us the possibility of representing the dynamic load effects by an equivalent static profile, say, the adopted as in the above-mentioned static tests.
2) There are many evaluation methods for the earthquake load effect. In these tests the peak values of acceleration were used for such a purpose. Here, the peak values are determined as 1.2 times of the fictitious yield accelerations based on the static strength. The results in Fig. 9 and 10 show that no collapse occurs under such a level of ground acceleration.
3) Whether the strength of the panel connections are strong or weak produce little effect on response behavior as shown in Fig. 10. The time histories are almost same in all tests, where two frames with the weak panels were tested. It should be emphasized that the static strength used as the basis of dynamic load effect evaluation must be calculated as precisely as possible, including the strain-hardening effect.

CONCLUDING REMARKS

The static tests and the on-line earthquake response tests on the frames of newly produced high strength steel show that the mechanical properties of the steel is suitable for building frames as the traditionally used mild steels.

ACKNOWLEDGEMENTS

The authors gratefully acknowledge the financial support of the Ministry of Education, Science and Culture, Grant-in-Aid for Scientific Research, No. 6346170. They wish to express their gratefulness for earnest cooperations offered by Mr. Y. Shimawaki and Mr. H. Kondo during the tests.

REFERENCES

1) Kuwamura, H., Ultimate Strength and Ductility of H-shaped Stub-columns of High Strength Steels with Different Yield Ratios, J. Structural Engineering Vol. 34B, 1988. 3, JSCE-AIJ

2) Takanashi, K. and Nakashima, M., Japanese Activities of On-line Testings, J. Engineering Mechanics, ASCE, Vol. 113, No.7, 1987. 7

Table 1 Mechanical properties of New HT60

	PL-9	PL-6
σ_Y (t/cm^2)	4.54	5.05
σ_u (t/cm^2)	6.35	6.40
YR(%)	72	79
EL(%)	17	19
ε_{st} (%)	0.58	1.2
E_{st}/E	1/70	1/90

Table 2 Section properties of members

	H-6	H-8	H-12
t_f (cm)	0.9	0.9	0.9
t_w (cm)	0.6	0.6	0.6
B (cm)	10.8	14.4	21.6
H (cm)	10.8	14.4	21.6
B/t_f	6	8	12
d/t_w	15	21	33
A(cm^2)	24.8	33.5	50.8
I_x (cm^4)	514	1280	4560
Z_P (cm^3)	110	200	473
M_P (t·cm)	504	923	2147
N_Y (t)	116	157	240

Table 3 Story shears at collapse

Test	Q_{u1} (t)	Q_{u2} (t)	Q_{u3} (t)
WBSC-W-1	10.2	8.5	5.1
WBSC-S-1	15.0	12.5	7.5
SBWC-W-1	15.0	12.5	7.5
SBWC-S-1	18.6	15.5	9.3

Table 5 Experimental parameters

Test	A_{max} (gal)	Q_u (ton)	M ton·s/cm	α
WBSC-W-2	500	14.5	0.0117	1.2
WBSC-S-2	606	18.8	0.0124	1.2
SBWC-W-2	343	20.6	0.024	1.2
SBWC-S-2	444	30.0	0.027	1.2

Table 4 Absorbed strain energy

Test	Ψ_1 (%)	Ψ_2 (%)	Ψ_3 (%)	W (ton·cm)
WBSC-W-1	33.6	41.7	25.7	346.7
WBSC-S-1	44.1	36.5	19.4	576.8
SBWC-W-1	36.7	39.0	24.3	646.9
SBWC-S-1	27.2	45.6	27.1	783.4

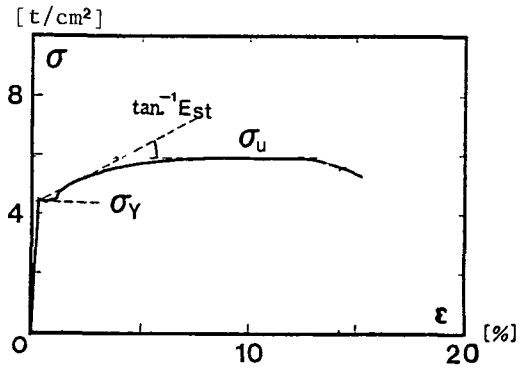

Fig.1 Stress-strain diagram of New HT60

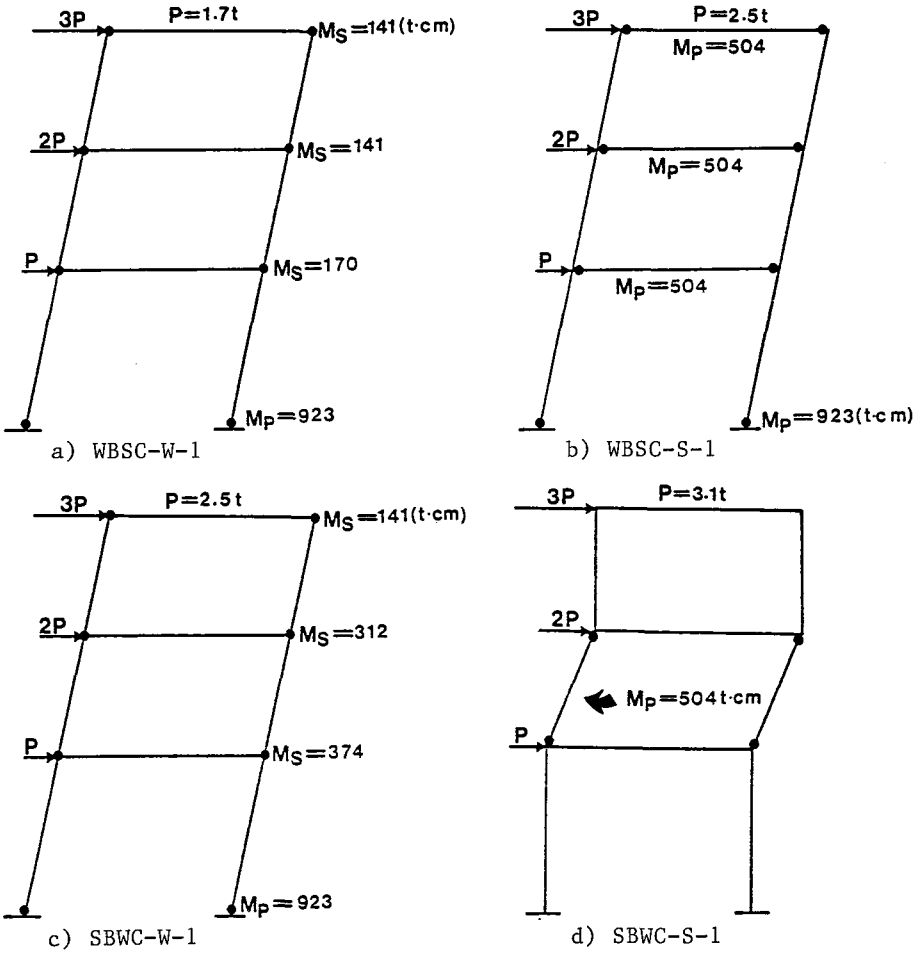

Fig.3 Collapse mechanisms associated with collapse loads

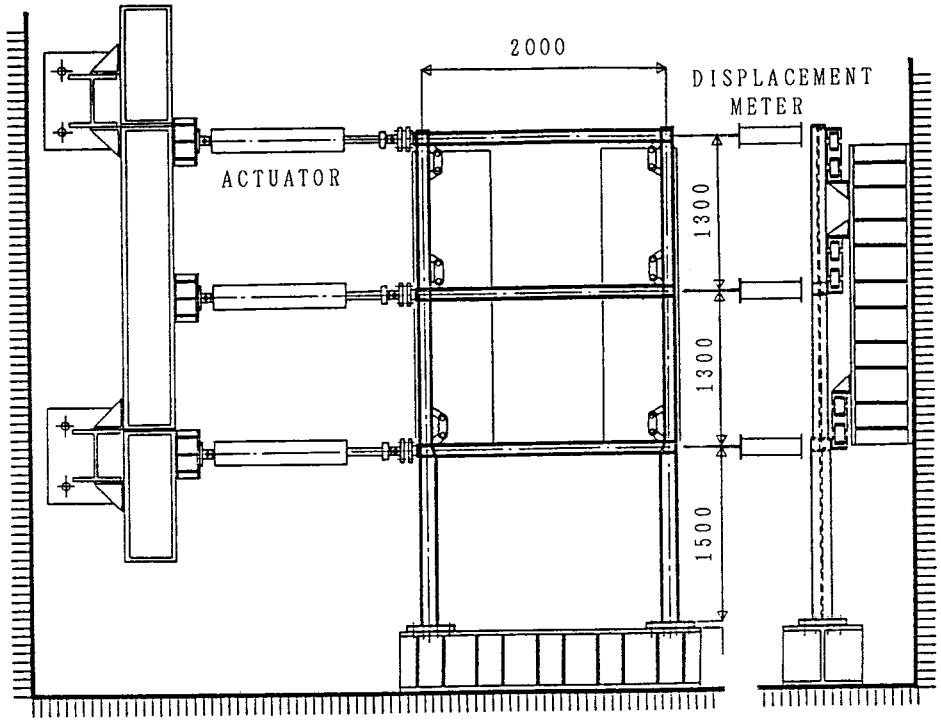

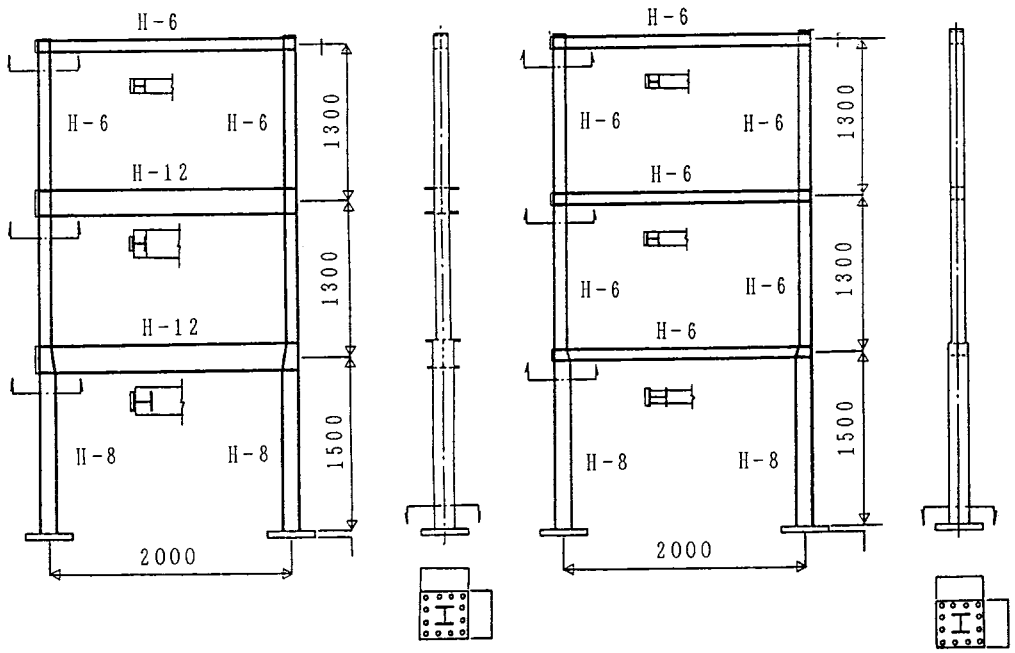

b) SBWC

a) WBSC

Fig.2 Test frames

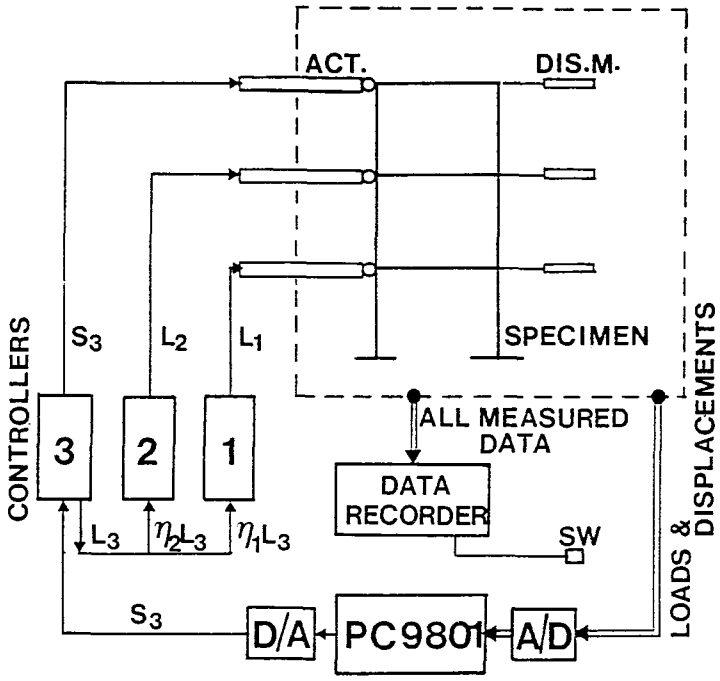

Fig.4 Loading system and data acquisition system (Static tests)

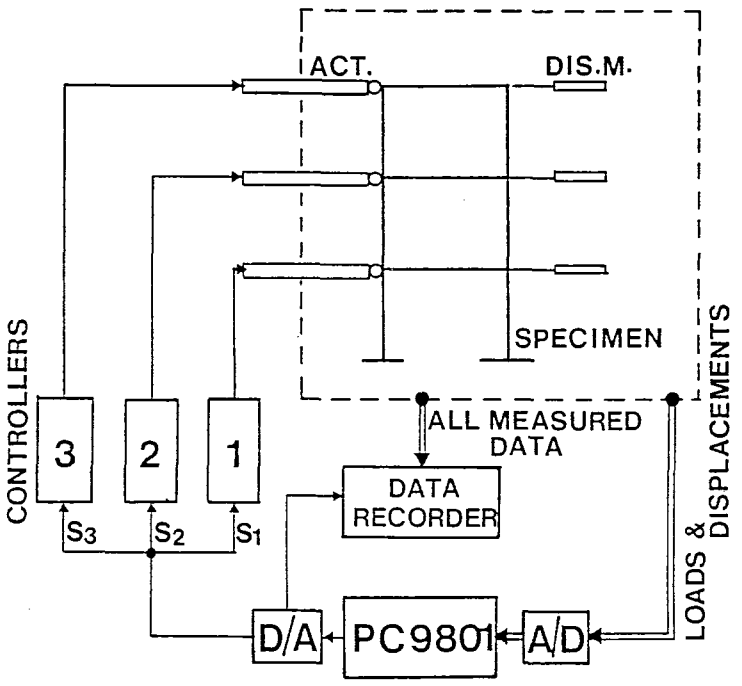

Fig.5 Loading system and data acquisition system
(On-line earthquake resposnse tests)

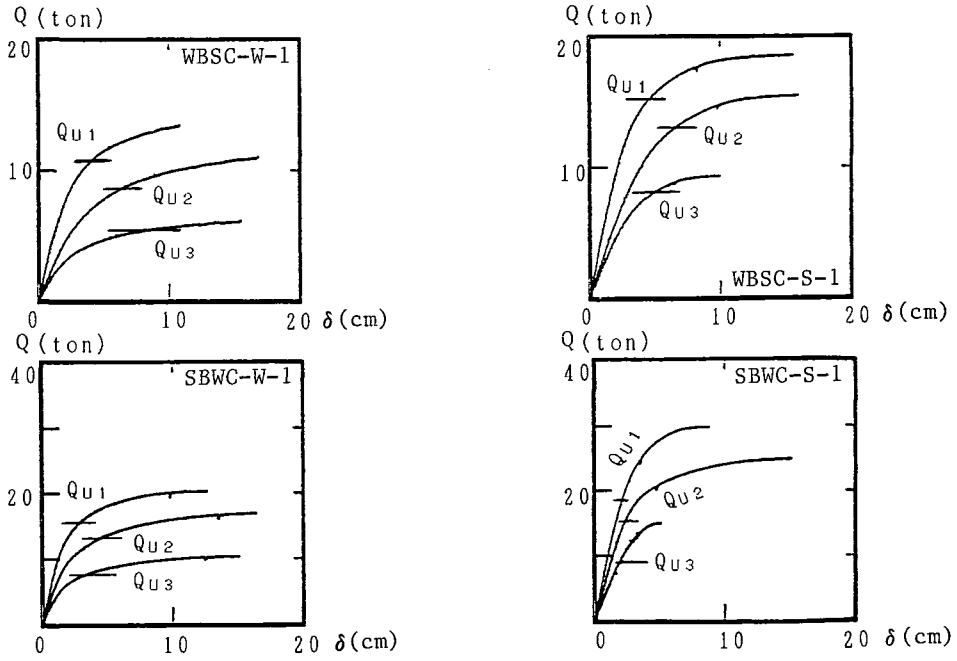

Fig.6 Story shear vs. story displacement relationship

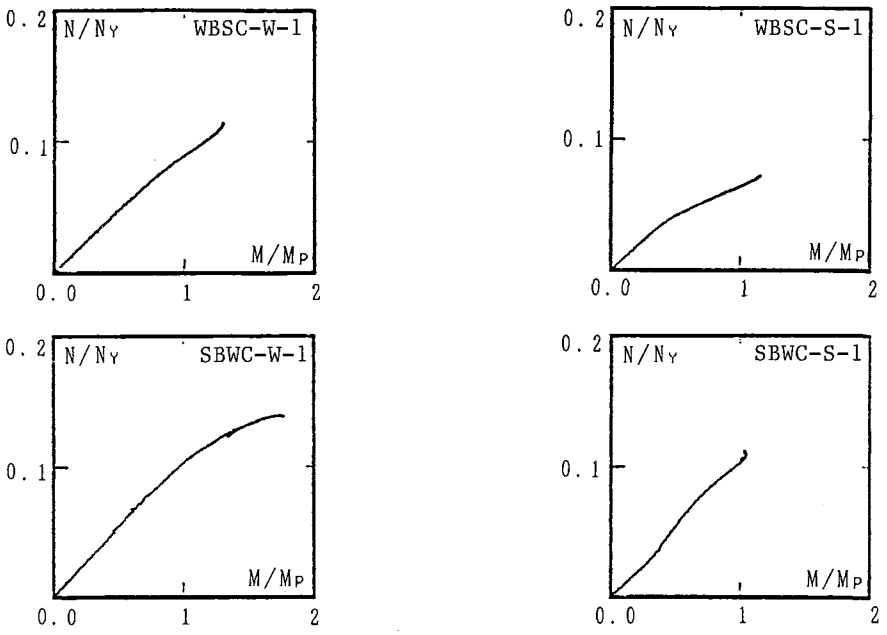

Fig.7 Bending moment vs. axial force relationships at column bases

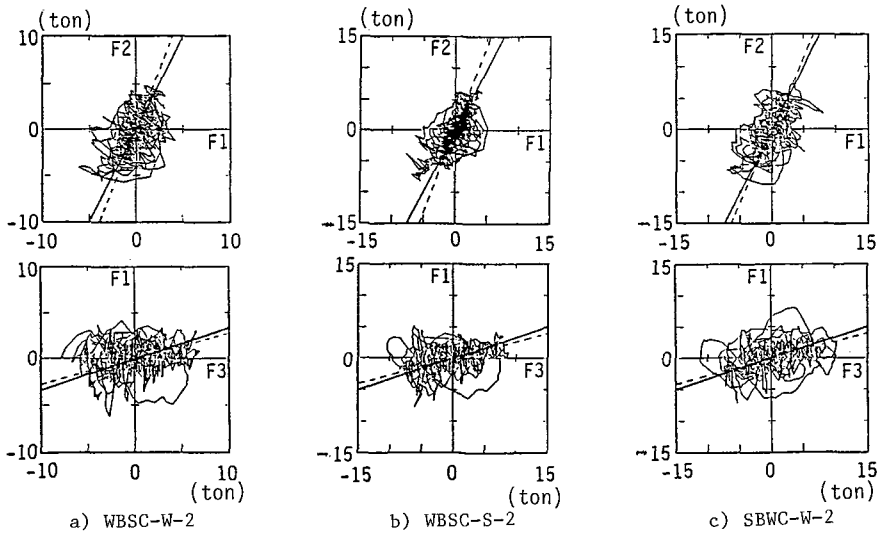

Fig.8 Trajectories of inertial forces at floor levels

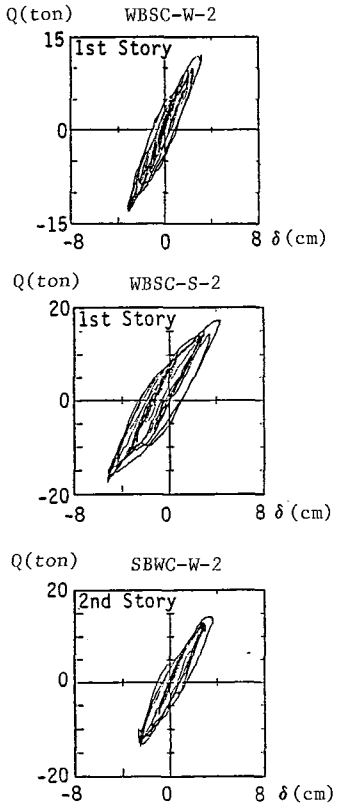

Fig.9 Story shear vs. story displacement relationships in on-line response tests

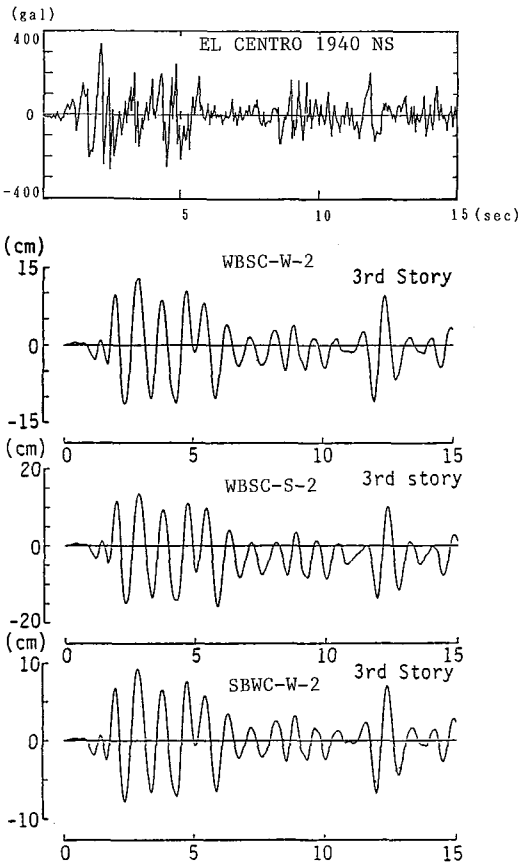

Fig.10 Time histories of response displacements